J Am Soc Nephrol 14: 2052–2062, 2003

Tissue Transglutaminase and the Progression of Human Renal Scarring

TIMOTHY S. JOHNSON,* AHMED F. EL-KORAIE,* N. JAMES SKILL,*‡ NAHED M. BADDOUR,† A. MEGUID EL NAHAS,* MELVIN NJLOMA,* AHMED G. ADAM,† and MARTIN GRIFFIN‡

**Sheffield Kidney Institute, Sheffield, and †Nottingham Trent University, Nottingham, United Kingdom; and ‡University of Alexandria, Alexandria, Egypt.*

Abstract. Experimental renal scarring indicates that tissue transglutaminase (tTg) may be associated with the accumulation of extracellular matrix (ECM), both indirectly via TGF-β1 activation and directly by the formation of $\epsilon(\gamma$-glutamyl) lysine dipeptide bonds within the ECM. The latter potentially accelerates deposition and confers the ECM with resistance to proteolytic digestion. Studied were 136 human renal biopsy samples from a range of chronic renal diseases (CRD) to determine changes in tTg and $\epsilon(\gamma$-glutamyl) lysine crosslinking. Immunofluorescence for insoluble tTg showed a 14-fold increase in the kidneys of CRD patients (5.3 $\pm$ 0.5 *versus* 76 $\pm$ 54 mV/cm^2), which was shown to be active by a similar 11-fold increase in the $\epsilon(\gamma$-glutamyl) lysine crosslink (1.8 $\pm$ 0.2 *versus* 19.3 $\pm$ 14.2 mV/cm^2). Correlations were obtained with renal function for tTg and crosslink. *In situ* hybridization for tTg mRNA showed that tubular epithelial cells were the major source of tTg; however, both mesangial and interstitial cells also contributed to elevated levels in CRD. This mRNA pattern was consistent with immunohistochemistry for soluble tTg. Changes in renal tTg and its product, the $\epsilon(\gamma$-glutamyl) lysine crosslink, occur in progressive renal scarring in humans independently of the original etiology and in a similar manner to experimental models. tTg may therefore play a role in the pathogenesis of renal scarring and fibrosis in patients with CRD and can therefore be considered a potential therapeutic target.

The progression of chronic renal failure is relentless in the majority of patients with chronic nephropathies. This is because of the underlying scarring process characterized by renal cell depletion and their replacement by extracellular matrix (ECM) (1). Research has established many pathways leading to both cellular loss and excessive and inappropriate deposition of ECM (1). Numerous mediators have been implicated, including proinflammatory cytokines and chemokines as well as profibrotic growth factors such as TGF-β1 (2). It is clear that these mediators influence key enzymatic pathways that play important roles in the regulation of cell and ECM turnover. This is the case, for instance, with TGF-β1 that is capable of both inhibiting cell proliferation as well as increasing the deposition of ECM through stimulating its synthesis and inhibiting collagenolytic activity (3). TGF-β1 is capable of inhibiting matrix metalloproteinase (MMP) and plasmin synthesis as well as inducing their inhibitors (tissue inhibitor of MMP [TIMP] and plasminogen activator inhibitor-1) (3). More recently, a role has been described for TGF-β1 in the modulation of another key ECM-modulating enzyme: tissue transglutaminase (tTg) (4). This enzyme may be linked to many of the actions of TGF-β1 in the scarred kidney, including loss of tubular cells and fibrosis.

tTg is a member of a family of enzymes that has the capacity to irreversibly crosslink proteins through a $\epsilon(\gamma$-glutamyl) lysine bond (5). Such action has been implicated in the crosslinking of ECM leading to increased deposition (6,7) and its resistance to proteolytic enzymes leading to tissue fibrosis (8). Recent studies in the remnant kidney model of renal scarring have shown that tTg is released by tubular cells and may have a multifunctional role in the progression of renal scarring (8,9). First, it moves to the extracellular environment, where the high Ca^{2+} and low Guanosine Triphosphate levels result in activation of the enzyme (10). This leads to the formation of ϵ-(γ-glutamyl) lysine dipeptide bonds within the ECM. This crosslinking may facilitate inappropriate deposition of ECM proteins (7,11) while instilling resistance to the action of MMP (8). Second, high intracellular levels of tTg can lead to a novel type of cell death by the crosslinking of cytoplasmic proteins after cell trauma and loss of Ca^{2+} homeostasis (12,13). This transglutaminase-associated cell death has been reported within the tubular compartment (9) and is independent of apoptosis, although tTg is also associated with cellular apoptosis (14–16). Cell deletion and tubular atrophy are major components of renal scarring and contribute to progressive renal insufficiency (17). Finally, tTg has also been shown to play a key role in the matrix storage and activation of TGF-β1, through the crosslinking of latent TGF-β1 binding protein to

Received November 20, 2002.Accepted March 31, 2003.
Correspondence to Dr. Tim Johnson, Sheffield Kidney Institute, Northern General Hospital Trust, Herries Road, Sheffield, S5 7AU, UK. Phone: +44 (0)114-2715322; Fax: +44(0) 114-2714410; E-mail: T.Johnson@sheffield.ac.uk

1046-6673/1408-2052
Journal of the American Society of Nephrology

DOI: 10.1097/01.ASN.0000079614.63463.DD

the ECM (18,19). Interestingly, TGF-β1 has also been shown to upregulate tTg transcription (4,20).

In this study, for the first time in human chronic renal disease (CRD), we investigated changes in tTg in progressive renal scarring by using biopsy material from patients with a variety of nephropathies and at different stages of the scarring process.

Materials and Methods

Patients

We retrospectively investigated renal biopsy material from 136 renal patients who had chronic renal diseases (CRD) due to a range of clinical and histologic diagnoses (CRD group) (Table 1). Chronic renal failure was defined as patients who were followed up for at least 6 mo at either institution with a serum creatinine level exceeding 1.5 mg/dl. These were compared with five renal samples obtained via biopsy from the healthy pole of nephrectomy specimens of patients with renal cell carcinoma (control group). Seventy of these biopsy samples were obtained from the Department of Histopathology, University Hospital of Alexandria, Egypt, between 1992 and 1997, and the remainder were retrieved from the archives of the Department of Histopathology, Sheffield Teaching Hospitals (Northern General Hospital Campus), United Kingdom, between 1994 and 1998.

Original histologic diagnoses were obtained from the patients' notes and substantiated by further examination of the biopsy samples by an independent pathologist (N.B.). All clinical information including renal function and proteinuria was obtained from either the patients' medical records or the unit's computerized patient database.

Immunohistochemistry and Immunofluorescence

Distribution of tTg and ϵ-(γ-Glutamyl) Lysine Crosslink. . The distribution of immunoreactive transglutaminase and its crosslink product, ϵ-(γ-glutamyl) lysine, was determined by immunolocalization on both neutral-buffered formalin-fixed, paraffin-embedded sections and unfixed cryostat sections. Paraffin-embedded fixed tissue is suitable for the detection of soluble tTg, but as a result of antibody exclusion/epitope occlusion on fixed tissue, the detection of insoluble tTg (attached to substrate, including ECM) is unsatisfactory for these sections. Instead, unfixed, frozen sections are used to detect insoluble tTg, although all soluble tTg is removed during the processing of these frozen sections and morphology is often difficult to evaluate. Thus, a combination of staining of fixed and unfixed tissue provides a comprehensive evaluation of tTg location.

tTg in Paraffin-Embedded Sections. Renal biopsy samples were fixed in 10% neutral buffered formalin, embedded in paraffin, and sectioned at 4 μm. Paraffin was removed and sections were rehydrated in descending grades of alcohol. After blocking of endogenous peroxidase activity with 3% H_2O_2 in methanol, antigen revealing was performed by Target Unmasking Fluid (ID Labs Biotechnology, Glasgow, UK) at 90°C for 10 min and at room temperature for another 10 min. Sections were blocked with antibody dilution buffer (3% w/v BSA, 0.05% vol/vol Triton X-100, PBS) plus 5% vol/vol goat serum for 1 h and then probed overnight at 4°C with 1:300 mouse anti-tTg (CUB7042) (Stratek Scientific, Luton, UK) in antibody dilution buffer plus 5% vol/vol goat serum. Antibody binding was revealed by an avidin-biotin technique using the ABC kit (Vector Laboratories, Peterborough, UK). Visualization of the reaction was performed with 3'amino-9'ethyl-carbimazole (AEC) (Vector Laboratories) as the chromogen.

tTg and ϵ-(γ-Glutamyl) Lysine in Unfixed Cryostat Sections. Unfixed cryostat sections were immunoprobed with either mouse monoclonal anti-tTg antibody (CUB7042) (Stratek Scientific) or mouse anti–ϵ-(γ-glutamyl) lysine monoclonal antibody (clone 81D4; Covalab, Lyon, France), as previously described (8). After fixing with −20°C methanol, primary antibody binding was revealed, either with the ABC kit (Vector Laboratories) with an AEC substrate for light microscopy, or with goat anti-mouse Cy5 (indodicarbocyanine)–conjugated antibody (Stratek Scientific) and visualized by confocal microscopy, as described previously (8).

Technique and Antibody Specificity. Technique specificity was determined by the replacement of the primary antibodies with an equal concentration of mouse nonimmune IgG. Both the monoclonal antibodies to tTg (CUB 7402) (13,21,22) and ϵ-(γ-glutamyl) lysine (clone 81D4) (23,24) have well characterized specificity; however, this was further confirmed by overnight preadsorption of the antisera with either purified tTg (Sigma, Poole, UK) or synthesized ϵ(γ-glutamyl) lysine (Bachem, UK). In neither case was any staining evident.

***In Situ* Transglutaminase Activity.** The determination of *in situ* transglutaminase activity was as described previously (8). Unfixed cryostat sections were incubated with FITC cadaverine (Molecular Probes, Leiden, The Netherlands) and $CaCl_2$. Negative controls included the replacement of $CaCl_2$ with EDTA or the addition of cystamine (Tg inhibitor) or CUB7042 (transglutaminase-inactivating

Table 1. Histopathologic diagnoses of patient biopsy samples

Pathologic Diagnoses	Proliferative (P) or Nonproliferative (NP)	Patient Group, *n* (%) (*n* = 136)	Control Group, *n* (%) (*n* = 5)
Amyloidosis	—	7 (5.1)	0 (0)
Crescentic glomerulonephritis (CGN)	P	5 (3.6)	0 (0)
Diabetic nephropathy (DN)	NP	4 (2.9)	0 (0)
End-stage renal disease (ESRD)	NP	38 (27.7)	0 (0)
Focal proliferative glomerulonephritis (FPGN)	P	3 (2.2)	0 (0)
Focal segmental glomerulosclerosis (FSGS)	NP	4 (2.9)	0 (0)
Mesangiocapillary glomerulonephritis (MCGN)	P	35 (25.5)	0 (0)
Membranous nephropathy (MN)	NP	14 (10.2)	0 (0)
Mesangial proliferative glomerulonephritis (including IgA nephropathy) (MPG)	P	21 (15.3)	0 (0)
Myeloma kidney	NP	2 (1.5)	0 (0)
Chronic pyelonephritis	NP	3 (2.2)	0 (0)

antibody) (Stratek Scientific). Positive controls were generated by the addition of 50 μg of purified tTg (Sigma) to the reaction buffer. After washing, fixing, and blocking, incorporated fluorescein cadaverine was revealed by immunoprobing with a mouse anti-FITC monoclonal antibody and visualized with a goat anti-mouse Cy5 conjugated antibody (Stratek Scientific). Sections were visualized by confocal microscopy (Leica DMRBE, Leica, Wetzlar, Germany) with a Kr-Ar laser at 650 nm (Cy5 optimal excitation). Computer imaging and analyses was obtained at emission wavelengths of 655 and 530 nm for Cy5 and autofluorescence, respectively.

***In Situ* Hybridization.** Formalin-fixed sections were rehydrated and digested with 5 μg/ml of proteinase K (Sigma) for 60 min at 37°C. These were then postfixed in 1% (wt/vol) paraformaldehyde and then probed with sense and antisense riboprobe constructs to tissue tTg constructed by using digoxigenin-labeled rUTP (Boehringer Ingelheim, Bracknell, UK) generated from the 375-bp *Bam*HI fragment of tTg via the riboprobe Gemini II system (Promega, Southampton, UK). Hybridization was performed at 50°C for 18 h in a 50% vol/vol formamide hybridization buffer containing 10 ng/ml of digoxigenin-labeled riboprobe. After stringency washes, any nonduplexed RNA was digested with 20 μg/ml RNase A (Sigma) for 30 min at 37°C. Binding of the riboprobes was then revealed by alkaline phosphatase–conjugated sheep antidigoxigenin antibody (Boehringer Ingelheim) with 4-nitro blue tetrazolium chloride/5-bromo-4-chloro-3-indoylphosphate used as the substrate (8).

Morphometric Analysis

All morphologic evaluations were performed separately by four of the authors blinded to the section code. A standard point counting method was used to quantitate Masson trichrome staining for the estimation of both glomerular sclerosis and interstitial fibrosis under a magnification of ×400 (25). The same method was used to quantitate bright field immunostaining for tTg and its crosslink product.

Twelve consecutive non-overlapping fields in the tubulointerstitium and all available glomeruli in the biopsy were evaluated using an 81 (9 × 9) point grid. The mean tubulointerstitium and glomerular scores per biopsy were evaluated as a percent of positive points to the total counted. Semi-quantitation by confocal microscopy was obtained directly using the emission intensity at 655 nm for both the tTg and the crosslink staining.

Semiquantitative Histomorphometric Analysis

Semiquantitative histomorphometric analysis was performed, with the parameters evaluated according to an arbitrary score (from 0 to +3) as described previously (9) for glomerular mesangial hypercellularity, tubular atrophy, and interstitial cellular infiltration.

Statistical Analyses

Results are given as mean and SD unless stated otherwise. Differences between the experimental groups were determined by the Kruskall-Wallis test followed by the Mann-Whitney *U* test or the Wilcoxon rank-sum test for *post hoc* comparison. Correlations between the different parameters were performed by Spearman's rank correlation test. Results were considered significant when the *P* value was less than 5%. All analysis was performed by SPSS statistical software and Microsoft Excel.

Results

Clinical Findings

The histologic classification and clinical characteristics of the CRD study groups are described in Tables 1 and 2, respectively. The majority (87%) of patients studied had impaired renal function (serum creatinine above 1.5 mg/dl). A significant proportion (92%) had proteinuria (>300 mg/24 h), with 79% having proteinuria greater than 1 g/24 h. Hypertension was present in 69.3% of patients. Eighty-four percent of patients had interstitial inflammation, with 53% of these having scores greater than 1 (Table 2). Control patients had normal serum creatinine at the time of the nephrectomy. None were known to have proteinuria or hypertension (Table 2). Glomerulosclerosis and interstitial fibrosis were significantly higher in all nephropathies compared with the control group. Interstitial inflammation was detected in 62% of the patients and none of the control biopsy samples (Table 2).

Immunohistochemistry

Soluble tTg Immunostaining. Detection of soluble tTg on formalin-fixed, paraffin-embedded sections showed little detectable staining in the normal kidney (Figure 1, A). Any immunostaining was predominantly in the glomerulus in a pattern that would be consistent with a mesangial distribution. Occasionally, some very faint staining was seen in the extracellular areas. In biopsy samples, increased immunostainable tTg was detected in both glomerular and tubular compartments (Figure 1, B through D). Glomerular staining appeared to be generally mesangial in nature (Figure 1, C) and was associated with areas of hypercellularity, with significant correlation between the two ($R^2 = 0.73$, $P < 0.001$). Some endothelial capillary lining also appeared to stain; however, this is difficult to conclusively distinguish in a damaged glomeruli. Changes in tubular staining occurred to a greater extent in the cortex (Figure 1, B and D), with

Table 2. Clinical data in control and patient groups[a]

Characteristic	Patient Group (mean ± SD)	Control Group (mean ± SD)	*P* Value
Age (yr)	41 ± 20	48.6 ± 10.8	< 0.001
Urea (mg/dl)	110.3 ± 99.1	32.4 ± 11.3	< 0.001
Serum creatinine (mg/dl)	4.1 ± 4.4	0.9 ± 0.5	< 0.001
MAP (mmHg)	108.6 ± 18.2	95.1 ± 5.8	< 0.001
24-h proteinuria (g/24 h)	3.1 ± 2.8	0.20.1	< 0.001
Glomerulosclerosis (%)	4.5 ± 3.4	0.4 ± 0.7	< 0.001
Interstitial fibrosis (%)	21.2 ± 10.9	3.8 ± 1.9	< 0.001
Mesangial cellularity (score 0 to 3)	1.9 ± 1.0	1.1 ± 0.8	< 0.001
Tubular atrophy (score 0 to 3)	1.32 ± 1.0	0.00 ± 0.00	< 0.001
Interstitial Inflammation (score 0 to 3)	1.03 ± 0.87	0.01 ± 0.01	< 0.001

[a] $n = 136$ and $n = 4$ for patient and control groups, respectively.

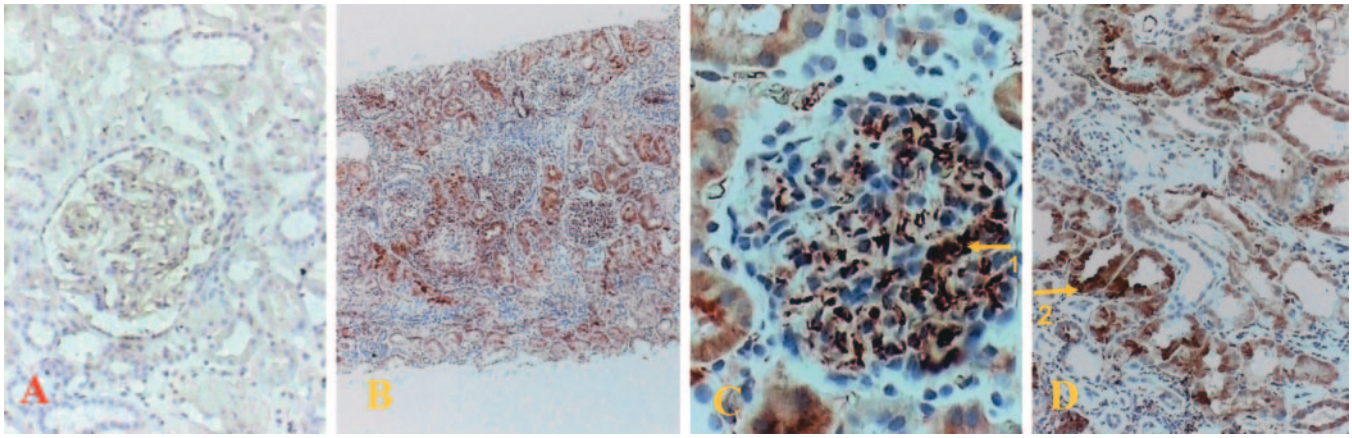

Figure 1. Representative photomicrographs of soluble tissue transglutaminase staining on fixed paraffin sections. (A) Control kidney. (B through D) Scarred kidneys showing increased staining, particularly in areas of hypercellularity in the mesangium (arrow 1) and in proximal tubule cells (arrow 2). Magnification: ×100 in A and B, ×400 in C (glomerular), and ×200 in D (cortex tubulointerstitium).

proximal and distal tubules the likely sources of tTg (Figure 1, B and D). Visualization of areas where tubular atrophy was less severe and renal architecture somewhat preserved indicates that although both cell types reveal elevated tTg, proximal tubular cells appeared to have stronger and more widespread immunostaining. This staining pattern was consistent regardless of the original histologic diagnosis.

Point counting analysis of soluble immunostainable tTg in the glomerular and tubulointerstitial compartments showed a 7.5-fold increase within the glomerulus and a 2.5-fold increase in tTg in the tubulointerstitium (Figure 2).

Insoluble tTg Immunostaining. Detection of insoluble tTg via both light (Figure 3) and confocal (Figure 4) microscopy on unfixed cryostat sections showed little staining in the normal kidney in either the glomeruli or tubulointerstitium (Figures 3 A, 4A, and 4B). In contrast, a marked increase in tTg immunostaining was seen in scarred kidneys. This was predominantly in the expanding tubulointerstitium (consistent with an extracellular staining pattern) and likely to be associated with the extracellular matrix (ECM) (Figures 3C, 3D, and 4C). Increases in glomerular staining were also significant, particularly in the periglomerular region (Figures 3B and 4D) but also throughout the mesangium. Changes in tTg staining in the mesangium were more evident by confocal microscopy (Figure 4, D) than light microscopy (Figure 3, B). The pattern of staining within both the glomeruli and tubulointerstitium again appeared to be independent of the original pathology.

ε-(γ-Glutamyl) Lysine Immunostaining. ε-(γ-Glutamyl) lysine staining provided a very similar immunostaining pattern to that of tTg. In normal kidneys, ε-(γ-glutamyl) lysine staining was minimal in either the glomerular or tubular compartments (Figure 4, E and F). Discrete and weak staining was noted in the glomerular mesangium and around the tubules. In diseased kidneys, extensive immunostaining was observed in the interstitium, which was particularly associated with extensive areas of scarring and fibrosis (Figure 4, G). This staining pattern appeared to be predominantly extracellular, although intracellular staining was also clearly visible. There was also a notable increase in the immunostaining for ε(γ-glutamyl) lysine crosslink within the mesangium (Figure 4, H).

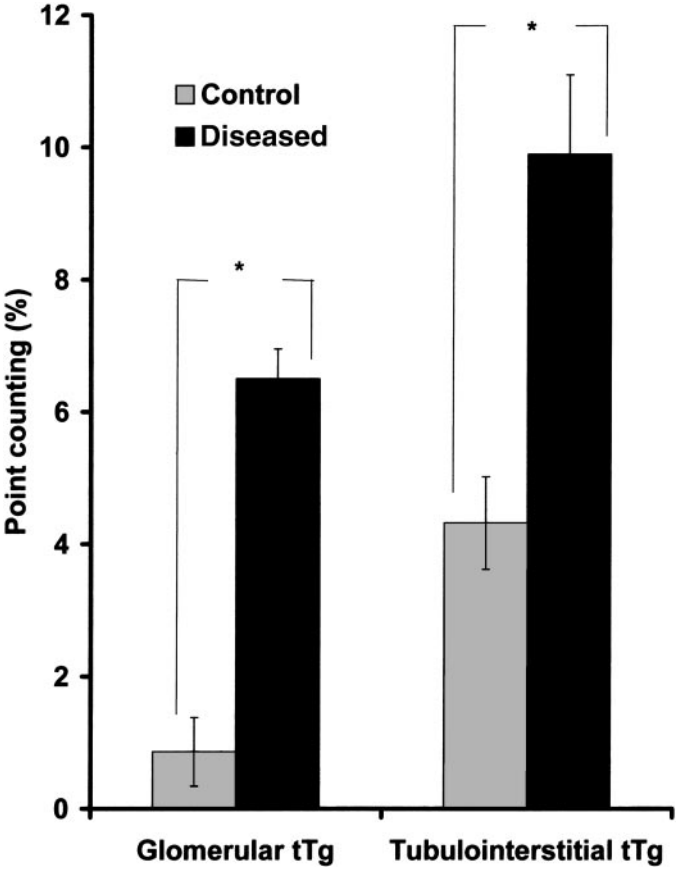

Figure 2. Bar graph illustrating point counting analysis (%) of soluble tissue transglutaminase (tTg) staining on fixed paraffin sections in both the tubular and glomerular compartments in diseased and normal biopsy tissue samples. Data represent mean point count score (%) ± SD. $n = 5$ for control and $n = 86$ for diseased samples. $^*P < 0.05$.

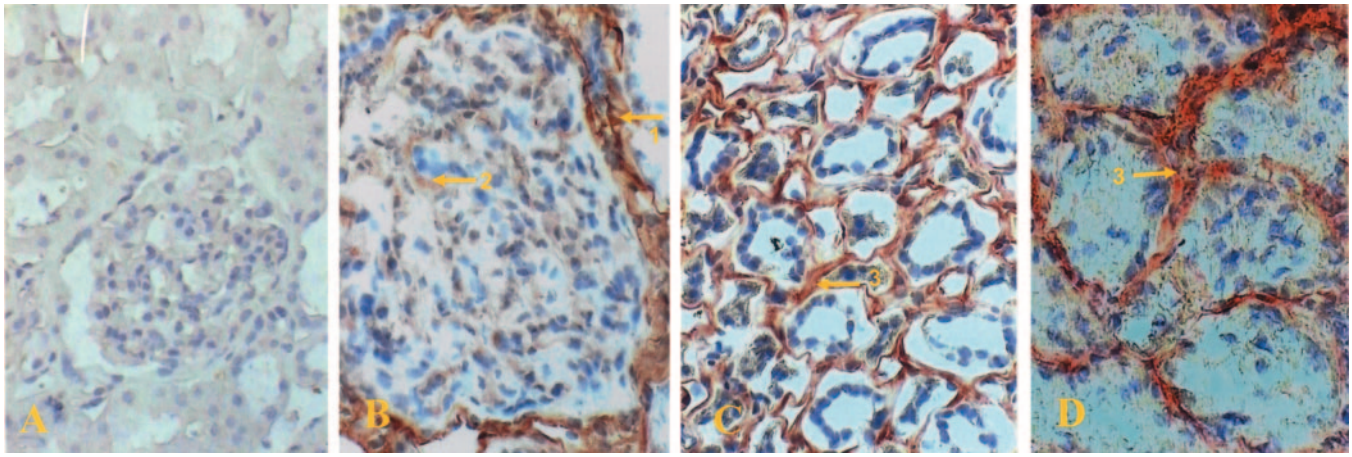

Figure 3. Representative pictographs of insoluble tissue transglutaminase staining on unfixed cryostat assessed by light microscopy. (A) Control kidney (magnification, ×100). (B through D) Diseased kidneys showing increased periglomerular (arrow 1), mesangial matrix (arrow 2), and interstitial (arrow 3) staining. Magnification, ×100 in A, ×400 in B (glomerular), ×200 in C (medulla tubulointerstitium), and ×400 in D (cortex tubulointerstitium).

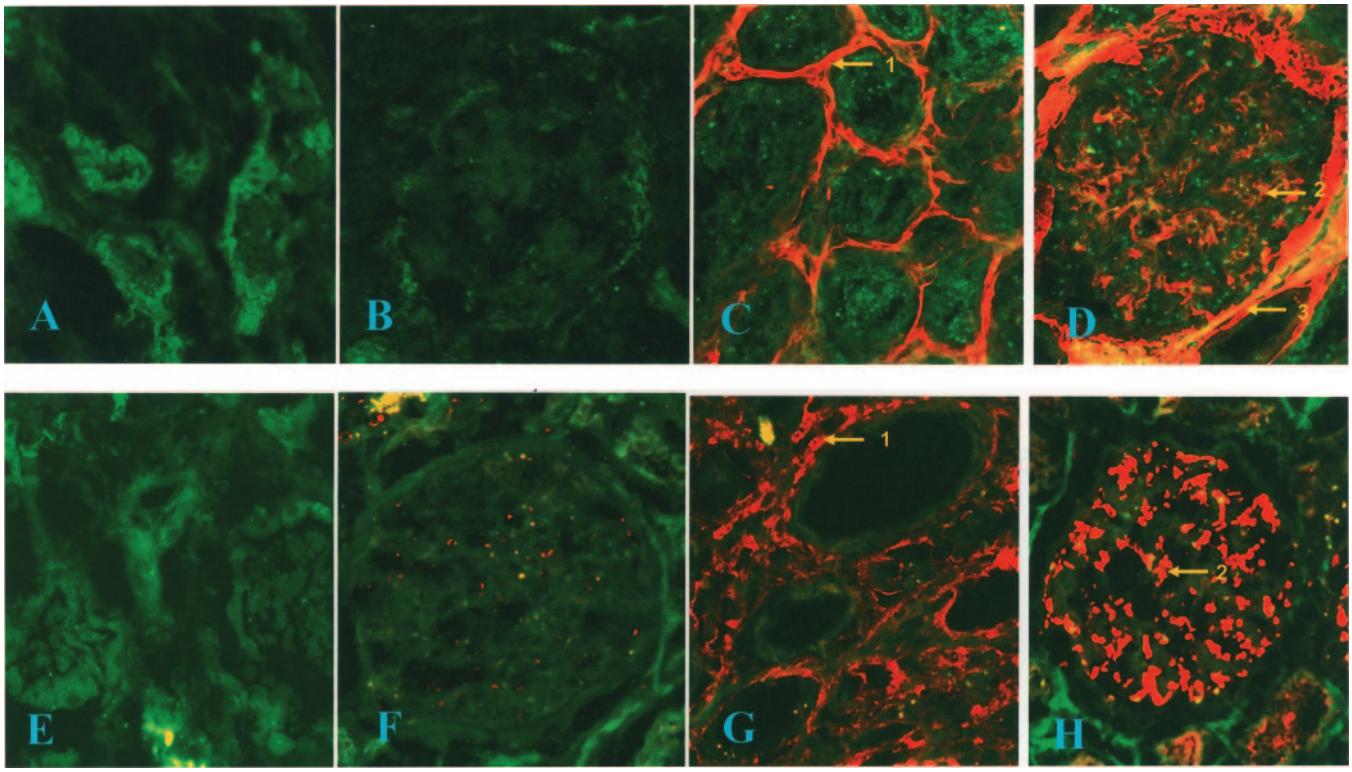

Figure 4. Representative photomicrographs of staining (Cy5; red) for insoluble tissue transglutaminase (tTg) and ε-(γ-glutamyl) lysine crosslink on unfixed cryostat sections assessed via confocal microscopy. (A through D) Stained for insoluble tTg. (E through H) Stained for crosslink. (A, B, E, F) Control kidneys. (C, D, G, H) Diseased kidneys showing increased staining in the expanded interstitium (arrow 1), the mesangium (arrow 2), and periglomerular (arrow 3). Magnification, ×400.

Quantitation of Insoluble tTg and ε-(γ-Glutamyl) Lysine

Semiquantitation of the overall insoluble tTg and ε-(γ-glutamyl) lysine crosslink staining by measuring the emission intensity of the Cy5 label at 665 nm by confocal microscopy revealed a significant increase in the diseased and scarred kidneys compared with controls when the data from the various pathologies were combined (Figure 5). This indicated a 14-fold increase in overall renal insoluble tTg staining and an 11-fold increase in ε-(γ-glutamyl) lysine crosslink staining. If tTg and ε-(γ-glutamyl) lysine crosslink immunostaining are broken down into individual disease states (Figure 5), it initially ap-

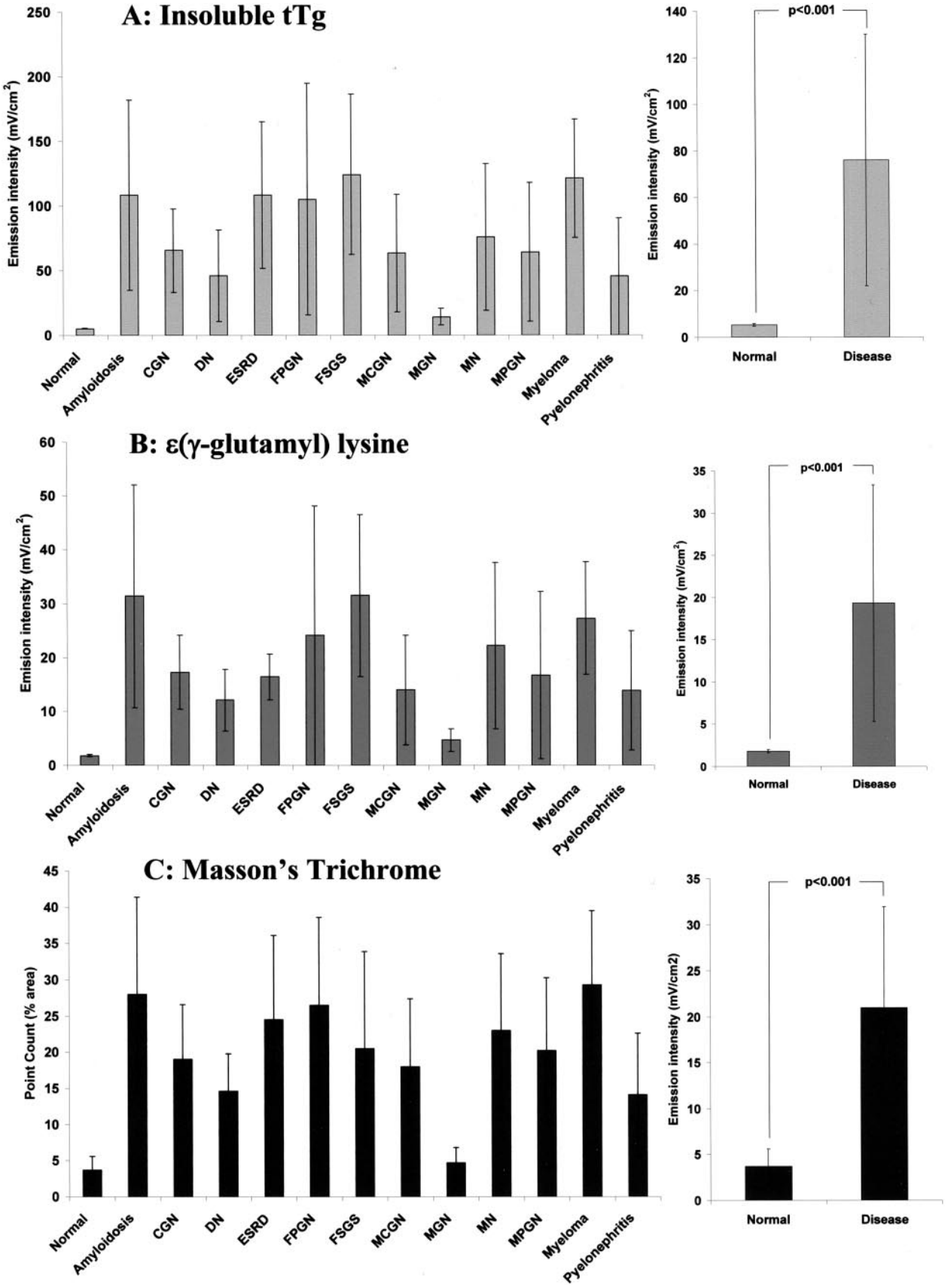

Figure 5. Semi-quantitation of whole biopsy insoluble tTg (A), crosslink (B), and Masson Trichrome staining (C) in normal and diseased kidney biopsies by diagnosis. tTg and crosslink were determined by confocal microscopy using Cy5 emission intensity at 665 nm and Masson Trichrome by point counting. Data represent mean ± SD. $n = 5$ for control and $n = 136$ for diseased biopsies.

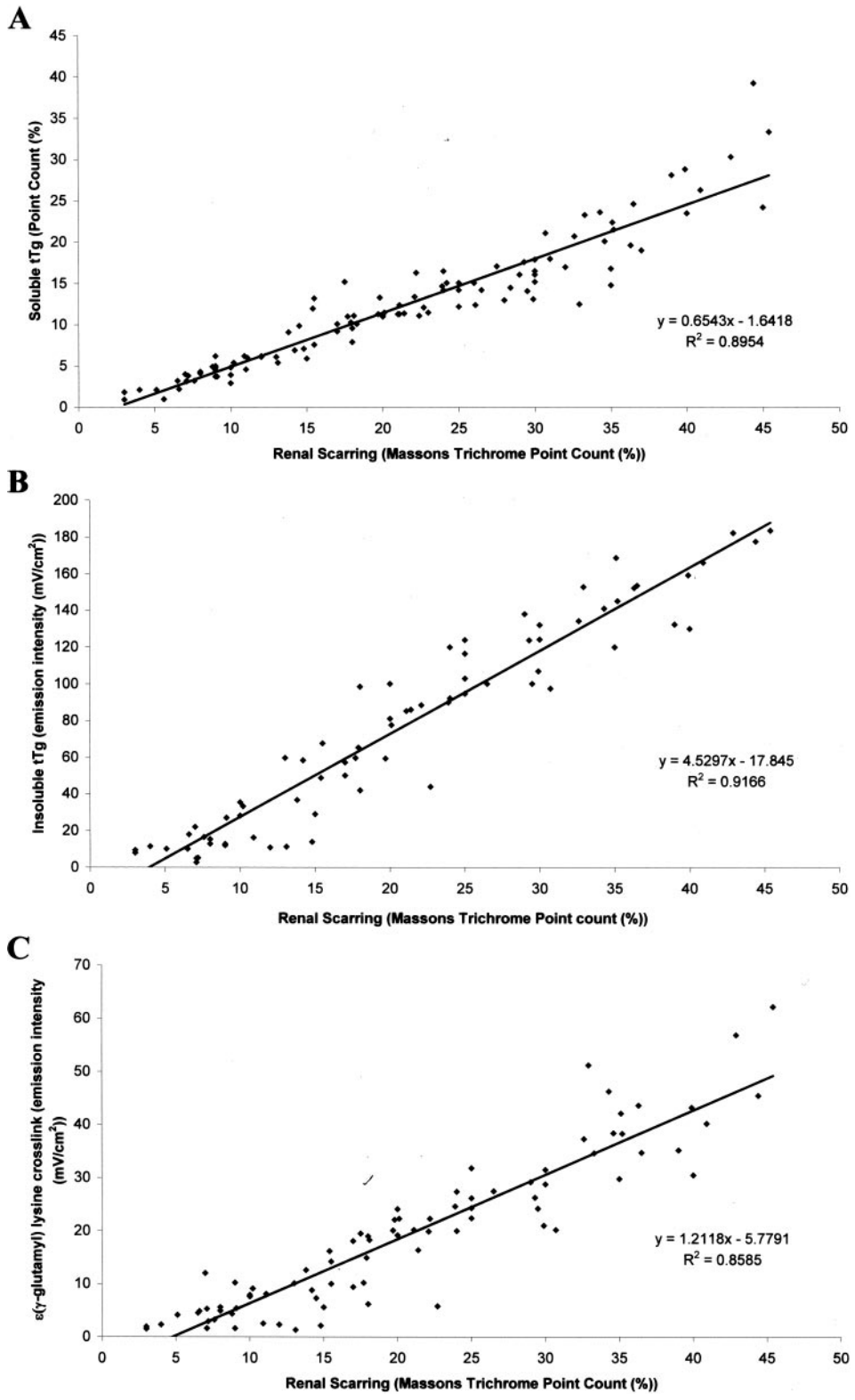

Figure 6. Correlation plots revealing an exceptionally high level of correlation with insoluble tTg and ϵ-(γ-glutamyl) lysine.

pears that certain conditions have considerably higher levels of tTg and ϵ-(γ-glutamyl) lysine crosslink staining than others. However, the use of point count analysis of Masson trichrome–stained sections as a measure of interstitial fibrosis clearly reveals large differences in the degree of scarring between the various pathologies. Consequently, disease entities exhibiting

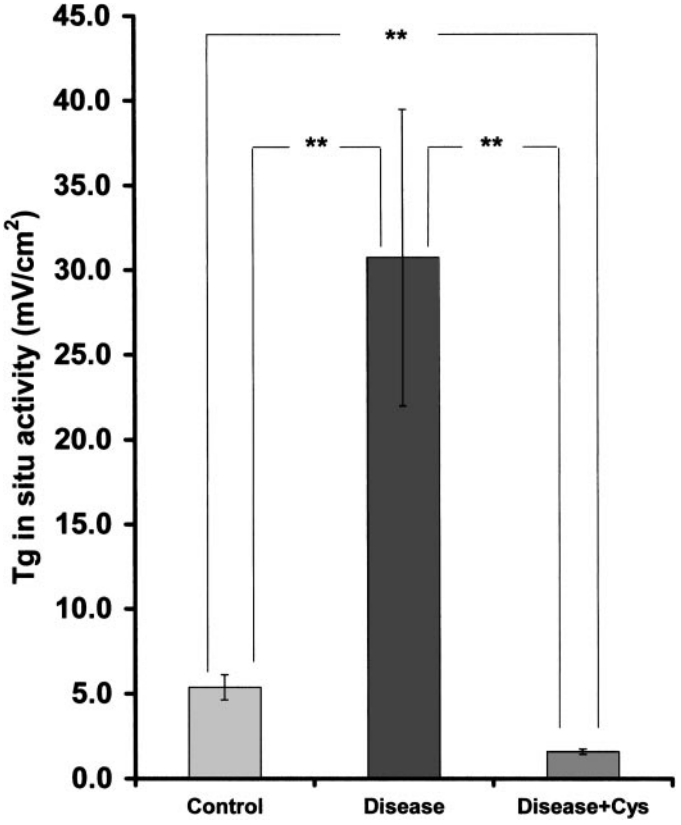

Figure 7. Bar graph revealing quantitation of whole-biopsy-sample *in situ* tissue transglutaminase activity by confocal microscopy by means of Cy5 emission intensity at 665 nm. Data represent mean Cy5 emission ± SD. $n = 3$ for control and $n = 33$ for diseased samples. Tg, transglutaminase; Cys, cystamine (Tg inhibitor).

higher levels of scarring also have higher levels of tTg and ε-(γ-glutamyl) lysine crosslink immunostaining. This demonstrates that differences in tTg and ε-(γ-glutamyl) lysine crosslinking between groups are dependent on the severity of renal scarring and the associated interstitial fibrosis.

tTg, ε-(γ-Glutamyl) Lysine, and Renal Scarring

To correct for the wide range of pathologic changes and severity seen within the renal biopsy samples of patients with CRD, a series of correlations with morphologic and functional parameters of disease progression was performed.

Tubulointerstitial fibrosis (Masson trichrome staining) showed an exceptionally high level of correlation with both insoluble tTg ($R^2 = 0.92$, $P < 0.001$) and ε-(γ-glutamyl) lysine ($R^2 = 0.86$, $P < 0.001$), as measured by emission intensity (Figure 6, B and C). When this correlation was repeated by using soluble tTg in the tubular compartment (point counted) against tubulointerstitial fibrosis, a similarly high ($R^2 = 0.89$, $P < 0.001$) correlation was noted (Figure 6, A). Correlations between total insoluble tTg and ε-(γ-glutamyl) lysine with tubular atrophy again were strongly positive ($R^2 = 0.69$ and 0.62, respectively $P < 0.01$).

Although we do not have specific confocal microscope measurement of glomerular staining for insoluble tTg and ε-(γ-glutamyl) lysine, when we correlated whole-kidney measurements of these parameters with glomerulosclerosis, we noted significant positive correlations (insoluble tTg, $R^2 = 0.56$, $P < 0.001$, and ε-(γ-glutamyl) lysine, $R^2 = 0.51$, $P < 0.001$). However, a higher correlation was detected between glomerular soluble tTg quantitated by point count analysis and glomerulosclerosis ($R^2 = 0.77$, $P < 0.05$). Subclassification of the diseases into proliferative and nonproliferative diseases showed better association of glomerulosclerosis in proliferative compared with nonproliferative conditions with soluble Tg, insoluble tTg, and ε-(γ-glutamyl) lysine (proliferative, $R^2 = 0.81$, 0.62, 0.58, all $P < 0.01$, *versus* nonproliferative, $R^2 = 0.43$, $P < 0.05$, 0.28 [NS], 0.29 [NS], respectively).

Interestingly, there was a strong correlation between mesangial proliferation and soluble glomerular tTg ($R^2 = 0.73$, $P < 0.001$), although this did not hold for ε-(γ-glutamyl) lysine and insoluble tTg. In proliferative diseases, there was a marginally better association of soluble tTg with mesangial proliferation than in nonproliferative diagnosis (0.76 *versus* 0.63, $P < 0.05$). This supports the observation of increased soluble tTg staining in areas of mesangial hypercellularity.

Correlating insoluble tTg and crosslink with serum creatinine showed some association ($R^2 = 0.46$, 0.47, respectively, $P < 0.05$), as did correlations with serum urea ($R^2 = 0.41$, 0.44, respectively, $P < 0.05$). When these two markers of function where correlated against soluble glomerular tTg, no significant correlation was noted.

Transglutaminase In Situ *Activity*

In 33 patient biopsy samples (amyloidosis 2, CGN 3, ESRD 8, FPGN 1, MCGN 9, MN 4, MPG 6) and five control samples, fluorescence from the incorporation of the labeled Tg substrate cadaverine was used to determine the level of Tg activity. This demonstrated a sixfold increase in insoluble Tg activity (Figure 7) that was inhibited by the addition of the Tg inhibitor cystamine. Localization of Tg activity was difficult because of loss of morphology during the procedure, but appeared to be consistent with that seen for insoluble tTg and crosslink (Figures 3 and 4). There was a significant correlation ($R^2 = 0.65$, $P < 0.01$) between Tg *in situ* activity and the level of interstitial fibrosis (Masson trichrome staining) (Figure 8) from mild to severe scarring.

tTg In Situ *Hybridization*

To determine whether the changes in tTg were mRNA dependent, we carried out *in situ* hybridization on 46 patient biopsy samples. In normal samples, tTg mRNA levels were below or on the threshold for detection (Figure 9, A and B); however, in scarred kidney, the tubular epithelial cells (Figure 9, C) and glomerular mesangial cells (Figure 9, E) showed a marked upregulation irrespective of the original etiology. A particularly striking visualization of tTg mRNA occurred in glomerular crescents (Figure 9, F). Some interstitial staining was observed (Figure 9, D) in most samples; however, it was not possible to assign it to a specific cell type.

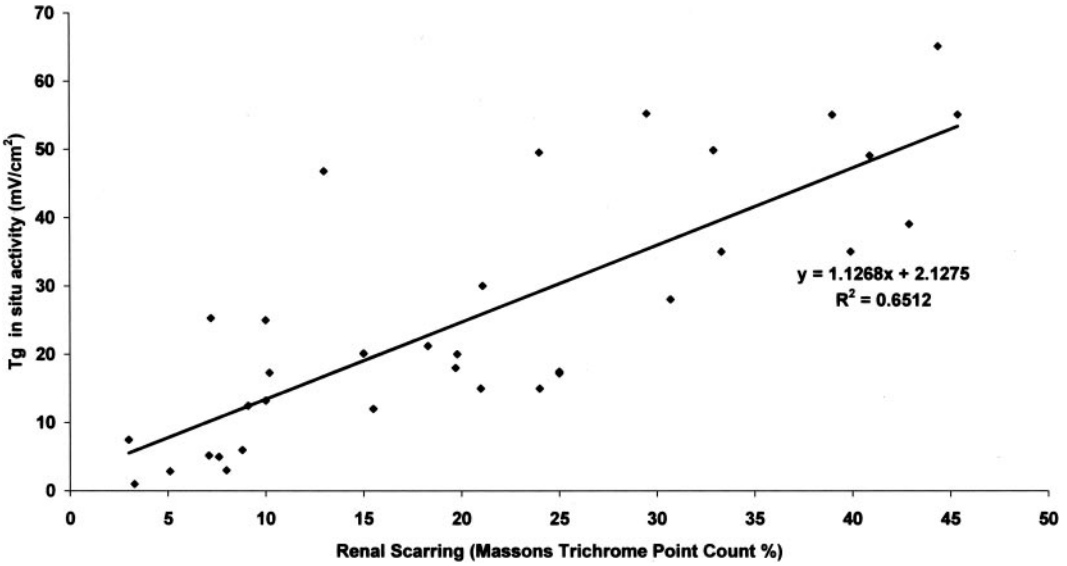

Figure 8. Correlation plot of interstitial fibrosis (Masson trichrome staining) in renal biopsy samples with transglutaminase *in situ* activity. Tg, transglutaminase.

Discussion

In the study presented here, we have investigated for the first time the association between tTg and the severity of renal scarring and fibrosis in patients with a range of etiologies. Previous studies conducted in experimental models of diabetic (26) and nondiabetic (8,9) renal scarring have implicated this enzyme in the crosslinking of the renal ECM, accelerating deposition and conferring resistance to the proteolytic activity of renal metalloproteinases (8). In addition, we have previously suggested that this enzyme may also contribute through intracellular cytoplasmic crosslinking to tubular cell death (9). Evidence presented here is based on the study of human nephropathies and demonstrates a strong association between renal fibrosis and the expression of tTg and its crosslink product, the $\epsilon(\gamma$-glutamyl) lysine isopeptide.

We have demonstrated an upregulation of soluble and insoluble tTg within the kidneys of patients who experienced a wide range of nephropathies in both the glomeruli and tubulointerstitium. As expected, the soluble component of the enzyme was primarily located intracellularly, whereas its insoluble counterpart was detected extracellularly in a periglomerular and peritubular distribution. The intracellular distribution of soluble tTg was predominantly within mesangial and tubular cells. In the mesangium, staining was more marked in areas of mesangial proliferation and hypercellularity. This was confirmed by a close correlation between mesangial cellularity scores and the intensity of the soluble tTg immunostain as measured by point counting, which were shown to be stronger in proliferative than nonproliferative disorders when diseases were subcharacterized. It is of note that the mesangial cells bear strong similarities to vascular smooth muscle cells (27). In addition, activation of mesangial cells is known to be associated with their transdifferentiation into a myofibroblastic phenotype sharing characteristics with smooth muscle cells and fibroblasts (28). Vascular injury and atherosclerosis associated with smooth muscle cell proliferation has been associated with the upregulation of tTg within these cells (29). Fibroblasts are also known to express tTg. It is therefore not too surprising that mesangial cell proliferation and activation are associated with an upregulation of this enzyme. Also, the upregulation of tTg expression and mRNA within glomerular epithelial crescents may reflect its synthesis by proliferating parietal epithelial cells, monocytes, or fibroblasts because all of these cell types have been detected within glomerular crescents and are known sources of tTg. In fact, many of these cells may originate from transdifferentiation of the glomerular epithelial cells themselves (30).

The precise role of tTg within proliferating, injured, or scarred glomeruli remains to be determined, although its regulation is likely a response to chronic cell trauma. One could speculate that the translocation of this enzyme into the extracellular mesangial space may play a role in the irreversible crosslinking of the collagenous mesangial matrix and may contribute to mesangial sclerosis that is often the forerunner of glomerulosclerosis. In support of this hypothesis, we detected both tTg and its crosslink product within mesangial areas, with a correlation between the amount of glomerular enzyme and glomerulosclerosis.

The tubular and peritubular distribution of tTg within diseased kidneys is reminiscent of our observations in the remnant kidneys of rats submitted to subtotal nephrectomy (8,9) and those with streptozotocin-induced diabetic nephropathy (26). It suggests similar mechanisms of action of tTg during the course of human renal scarring compared with that of experimental animals, including intracellular upregulation of the enzyme, its extracellular translocation, and its crosslinking of substrates in a peritubular and periglomerular distribution suggestive of an ECM target. In the periglomerular and peritubular spaces, the distribution of the enzyme is similar to that of myofibroblasts as well as the deposited ECM. Fibroblasts are known to release tTg, and ECM is known to bind the enzyme and act as a substrate for its crosslinking activity (7,11,31,32). However,

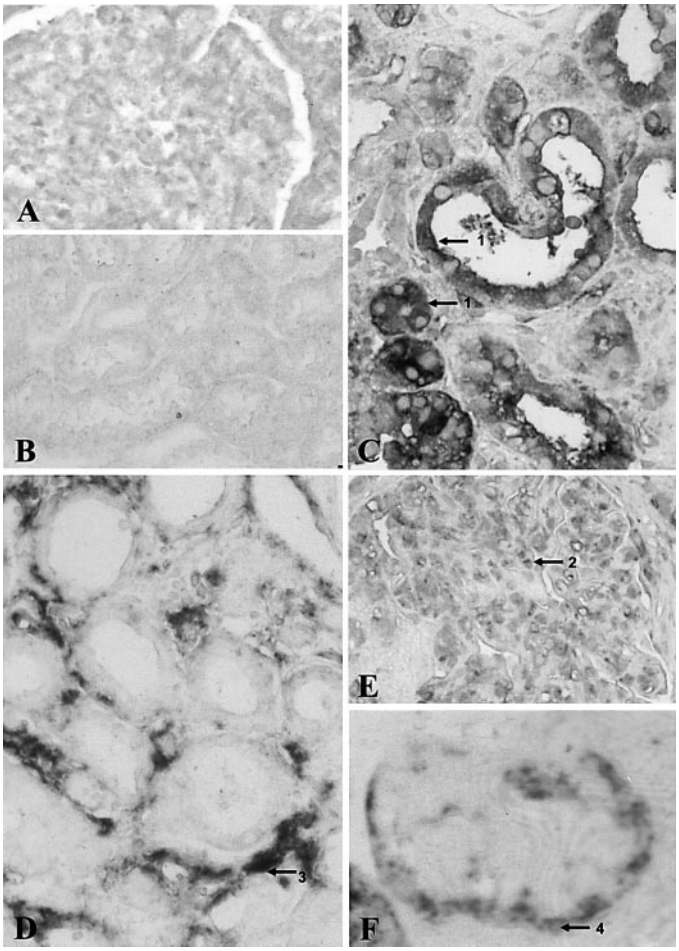

Figure 9. In situ hybridization for tissue transglutaminase mRNA in (A, B) normal and (C through F) diseased kidneys emphasizing regulation in epithelial (arrows 1), mesangial (arrow 2), and interstitial (arrow 3) cells. Strong staining was noted in glomerular crescents (arrow 4). Magnification, ×400 in A, E, and F, ×100 in B, and ×200 in C and D.

although we show increased mRNA expression in the interstitial cells that was noticeably greater than in remnant kidneys, the contribution of this toward the total tTg pool is still minimal when compared with that of tubular cells (8,9). Therefore, although myofibroblasts may contribute significantly to the level of ECM components available for deposition during renal scarring (33–35), it is the perturbation of tTg production and its release by tubular cells that is likely to lead to the enhanced levels of $\epsilon(\gamma$-glutamyl) lysine found in the ECM both in human as well as in experimental scarring (8,9). Of particular relevance is the observed close association and correlation between tTg and interstitial fibrosis, with an extremely high predictive value for the presence of tTg extracellular crosslink products and that of histologic abnormality. This may merely reflect the binding of this enzyme to the ECM as well as a possible pathogenic role in the development of renal fibrosis.

Finally, interstitial fibrosis is often associated with a heavy monocytic infiltrate. Monocytes are also known to be a source of tTg (36) and may therefore contribute to the pool of interstitial cells producing this enzyme and contributing to interstitial fibrosis. A close temporal association is known to take place between interstitial monocytic infiltration and interstitial fibrosis (1). This may reflect that monocytic tTg has been ascribed roles in latent TGF-β1 activation during inflammation and scarring (37), receptor-mediated endocytosis (38), and the adhesion and migration of monocytes (39).

tTg is potentially a potent fibrogenic enzyme capable of contributing to increased ECM deposition via a mechanism involving inter molecular crosslinking of matrix proteins leading to resistant to MMP and collagenases (7,8,40). This enzyme also has the capacity to bind TGF-β1 to ECM and the cell surface, thus facilitating its activation (18,19,41). The high correlation of both tTg and $\epsilon(\gamma$-glutamyl) lysine to disease progression that is irrelevant of etiology coupled with our development of urine assays makes these ideal candidates for noninvasive markers of renal scarring. In this study, we provide strong evidence to support the hypothesis that tTg is associated with progressive scarring and fibrosis in human renal disease and that tTg and $\epsilon(\gamma$-glutamyl) lysine are potential biochemical markers of chronic renal scarring.

Acknowledgments

This work has been supported by the award of a National Kidney Research Fund (UK) Senior Fellowship to T.S.J. (SF/2/2000), the Sheffield Kidney Research Foundation, and the Egyptian government.

References

1. Eddy AA: Molecular basis of renal fibrosis. *Pediatr Nephrol* 15: 290–301, 2000
2. Fogo AB: Glomerular hypertension, abnormal glomerular growth, and progression of renal diseases. *Kidney Int Suppl* 75: S15–S21, 2000
3. Basile DP: The transforming growth factor beta system in kidney disease and repair: Recent progress and future directions. *Curr Opin Nephrol Hypertens* 8: 21–30, 1999
4. Douthwaite JA, Johnson TS, Haylor JL, Watson P, El Nahas AM: Effects of transforming growth factor-beta1 on renal extracellular matrix components and their regulating proteins. *J Am Soc Nephrol* 10: 2109–2119, 1999
5. Lorand L, Conrad SM: Transglutaminases. *Mol Cell Biochem* 58: 9–35, 1984
6. Mirza A, Liu SL, Frizell E, Zhu J, Maddukuri S, Martinez J, Davies P, Schwarting R, Norton P, Zern MA: A role for tissue transglutaminase in hepatic injury and fibrogenesis, and its regulation by NF-kappaB. *Am J Physiol* 272: G281–G288, 1997
7. Kleman JP, Aeschlimann D, Paulsson M, van der Rest M: Transglutaminase-catalyzed cross-linking of fibrils of collagen V/XI in A204 rhabdomyosarcoma cells. *Biochemistry* 34: 13768–13775, 1995
8. Johnson TS, Skill NJ, El Nahas AM, Oldroyd SD, Thomas GL, Douthwaite JA, Haylor JL, Griffin M: Transglutaminase transcription and antigen translocation in experimental renal scarring. *J Am Soc Nephrol* 10: 2146–2157, 1999
9. Johnson TS, Griffin M, Thomas GL, Skill J, Cox A, Yang B, Nicholas B, Birckbichler PJ, Muchaneta-Kubara C, Meguid El Nahas A: The role of transglutaminase in the rat subtotal nephrectomy model of renal fibrosis. *J Clin Invest* 99: 2950–2960, 1997

10. Smethurst PA, Griffin M: Measurement of tissue transglutaminase activity in a permeabilized cell system: Its regulation by Ca^{2+} and nucleotides. *Biochem J* 313: 803–808, 1996
11. Aeschlimann D, Paulsson M: Cross-linking of laminin-nidogen complexes by tissue transglutaminase: A novel mechanism for basement membrane stabilization. *J Biol Chem* 266: 15308–15317, 1991
12. Johnson TS, Scholfield CI, Parry J, Griffin M: Induction of tissue transglutaminase by dexamethasone: Its correlation to receptor number and transglutaminase-mediated cell death in a series of malignant hamster fibrosarcomas. *Biochem J* 331: 105–112, 1998
13. Verderio E, Nicholas B, Gross S, Griffin M: Regulated expression of tissue transglutaminase in Swiss 3T3 fibroblasts: Effects on the processing of fibronectin, cell attachment, and cell death. *Exp Cell Res* 239: 119–138, 1998
14. Knight RL, Hand D, Piacentini M, Griffin M: Characterization of the transglutaminase-mediated large molecular weight polymer from rat liver: Its relationship to apoptosis. *Eur J Cell Biol* 60: 210–216, 1993
15. Knight CR, Rees RC, Griffin M: Apoptosis: A potential role for cytosolic transglutaminase and its importance in tumour progression. *Biochim Biophys Acta* 1096: 312–318, 1991
16. Fesus L, Thomazy V, Falus A: Induction and activation of tissue transglutaminase during programmed cell death. *FEBS Lett* 224: 104–108, 1987
17. Thomas GL, Yang B, Wagner BE, Savill J, El Nahas AM: Cellular apoptosis and proliferation in experimental renal fibrosis. *Nephrol Dial Transplant* 13: 2216–2226, 1998
18. Nunes I, Gleizes PE, Metz CN, Rifkin DB: Latent transforming growth factor-beta binding protein domains involved in activation and transglutaminase-dependent cross-linking of latent transforming growth factor-beta. *J Cell Biol* 136: 1151–1163, 1997
19. Verderio E, Gaudry C, Gross S, Smith C, Downes S, Griffin M: Regulation of cell surface tissue transglutaminase: Effects on matrix storage of latent transforming growth factor-beta binding protein-1. *J Histochem Cytochem* 47: 1417–1432, 1999
20. George MD, Vollberg TM, Floyd EE, Stein JP, Jetten AM: Regulation of transglutaminase type II by transforming growth factor-beta 1 in normal and transformed human epidermal keratinocytes. *J Biol Chem* 265: 11098–11104, 1990
21. Gaudry CA, Verderio E, Aeschlimann D, Cox A, Smith C, Griffin M: Cell surface localization of tissue transglutaminase is dependent on a fibronectin-binding site in its N-terminal beta-sandwich domain. *J Biol Chem* 274: 30707–30714, 1999
22. Birckbichler PJ, Upchurch HF, Patterson MK Jr, Conway E: A monoclonal antibody to cellular transglutaminase. *Hybridoma* 4: 179–186, 1985
23. Roch AM, Noel P, el Alaoui S, Charlot C, Quash G: Differential expression of isopeptide bonds N epsilon (gamma-glutamyl) lysine in benign and malignant human breast lesions: An immunohistochemical study. *Int J Cancer* 48: 215–220, 1991
24. el Alaoui S, Legastelois S, Roch AM, Chantepie J, Quash G: Transglutaminase activity and N epsilon (gamma glutamyl) lysine isopeptide levels during cell growth: An enzymic and immunological study. *Int J Cancer* 48: 221–226, 1991
25. Yang B, Johnson TS, Thomas GL, Watson PF, Wagner B, Skill NJ, Haylor JL, El Nahas AM: Expression of apoptosis-related genes and proteins in experimental chronic renal scarring. *J Am Soc Nephrol* 12: 275–288, 2001
26. Skill NJ, Griffin M, El Nahas AM, Sanai T, Haylor JL, Fisher M, Jamie MF, Mould NN, Johnson TS: Increases in renal epsilon-(gamma-glutamyl)-lysine crosslinks result from compartment-specific changes in tissue transglutaminase in early experimental diabetic nephropathy: Pathologic implications. *Lab Invest* 81: 705–716, 2001
27. Kreisberg JI, Venkatachalam M, Troyer D: Contractile properties of cultured glomerular mesangial cells. *Am J Physiol* 249: F457–F463, 1985
28. Johnson RJ, Floege J, Yoshimura A, Iida H, Couser WG, Alpers CE: The activated mesangial cell: A glomerular "myofibroblast"? *J Am Soc Nephrol* 2: S190, S197, 1992
29. Bowness JM, Venditti M, Tarr AH, Taylor JR: Increase in epsilon(gamma-glutamyl)lysine crosslinks in atherosclerotic aortas. *Atherosclerosis* 111: 247–253, 1994
30. Ng YY, Fan JM, Mu W, Nikolic-Paterson DJ, Yang WC, Huang TP, Atkins RC, Lan HY: Glomerular epithelial-myofibroblast transdifferentiation in the evolution of glomerular crescent formation. *Nephrol Dial Transplant* 14: 2860–2872, 1999
31. Bowness JM, Folk JE, Timpl R: Identification of a substrate site for liver transglutaminase on the aminopropeptide of type III collagen. *J Biol Chem* 262: 1022–1024, 1987
32. Martinez J, Chalupowicz DG, Roush RK, Sheth A, Barsigian C: Transglutaminase-mediated processing of fibronectin by endothelial cell monolayers. *Biochemistry* 33: 2538–2545, 1994
33. Goumenos DS, Tsamandas AC, Oldroyd S, Sotsiou F, Tsakas S, Petropoulou C, Bonikos D, El Nahas AM, Vlachojannis JG: Transforming growth factor-beta(1) and myofibroblasts: A potential pathway towards renal scarring in human glomerular disease. *Nephron* 87: 240–248, 2001
34. Goumenos D, Tsomi K, Iatrou C, Oldroyd S, Sungur A, Papaioannides D, Moustakas G, Ziroyannis P, Mountokalakis T, El Nahas AM: Myofibroblasts and the progression of crescentic glomerulonephritis. *Nephrol Dial Transplant* 13: 1652–1661, 1998
35. Goumenos DS, Brown CB, Shortland J, el Nahas AM: Myofibroblasts, predictors of progression of mesangial IgA nephropathy? *Nephrol Dial Transplant* 9: 1418–1425, 1994
36. Seiving B, Ohlsson K, Linder C, Stenberg P: Transglutaminase differentiation during maturation of human blood monocytes to macrophages. *Eur J Haematol* 46: 263–271, 1991
37. Gosiewska A, Yi CF, Blanc-Brude O, Geesin JC: Characterization of a macrophage-based system for studying the activation of latent TGF-beta. *Methods Cell Sci* 21: 47–56, 1999
38. Abe S, Yamashita K, Kohno H, Ohkubo Y: Involvement of transglutaminase in the receptor-mediated endocytosis of mouse peritoneal macrophages. *Biol Pharm Bull* 23: 1511–1513, 2000
39. Akimov SS, Belkin AM: Cell surface tissue transglutaminase is involved in adhesion and migration of monocytic cells on fibronectin. *Blood* 98: 1567–1576, 2001
40. Greenberg C, Birckbichler P, Rice R: Transglutaminases: Multifunctional enzymes that stabilise tissues. *FEBS Letts* 5: 3071–3077, 1991
41. Kojima S, Nara K, Rifkin DB: Requirement for transglutaminase in the activation of latent transforming growth factor-beta in bovine endothelial cells. *J Cell Biol* 121: 439–448, 1993